

# Diffusivity and Viscosity of Concentrated Hydrogenated Polybutadiene Solutions

Hui Tao and Timothy P. Lodge\*

Department of Chemistry, University of Minnesota, Minneapolis, Minnesota 55455-0431

Ernst D. von Meerwall

Department of Physics and Institute of Polymer Science, University of Akron, Akron, Ohio 44325-4001

Received November 24, 1999; Revised Manuscript Received January 11, 2000

**ABSTRACT:** We report measurements of diffusion ( $D$ ) and viscosity ( $\eta$ ) in hydrogenated polybutadiene (hPB)/alkane solutions. The volume fractions ( $\phi$ ) extend from 0.20 up to the melt and the molecular weights ( $M$ ) from 4900 up to 440 000; the number of entanglements per chain,  $M/M_e$ , ranges up to about 450. The temperature dependences of both  $D$  and  $\eta$  are similar, consistent with literature values, and independent of  $\phi$  and  $M$ . We thus conclude that the monomeric friction factor is also independent of  $\phi$  and  $M$ . For all samples with  $M/M_e \geq 3$  the data are consistent with the scaling relations  $D \sim M^{-2.4 \pm 0.1} \phi^{-1.8 \pm 0.2}$  and  $\eta \sim M^{3.4 \pm 0.1} \phi^{3.8 \pm 0.2}$ ; within the precision of the data the  $M$  exponents do not depend on  $\phi$ , and the  $\phi$  exponents do not depend on  $M$ . The  $M$  exponent for  $D$  in solution is consistent with previously reported studies for  $\phi \leq 0.4$  but apparently conflicts with the reptation value of  $-2.0$  in the melt. However, by comparing with the literature melt self-diffusion data for hPB and six other polymers, it is clear that the exponent is, in fact, universally stronger than  $-2.0$ . Furthermore, if a single universal exponent is assumed, the best value based on all the data is  $-2.28 \pm 0.05$ . Our hPB data resolve the longstanding anomaly that the longest relaxation times  $\tau_1$  based on translation ( $\sim R_g^2/D$ ) and orientational relaxation ( $\sim \eta$ ) appeared to have different  $M$  dependences. The data also indicate that for both solutions and melts the dynamics are determined primarily by the number of entanglements per chain. The data are compared with current models of polymer dynamics, both reptative and nonreptative. In the former case it is clear that a self-consistent theory incorporating both "constraint release" and "contour length fluctuations" is required.

## Introduction

The dynamics of entangled polymer liquids have been a topic of great interest in recent years, in large measure stimulated by the advent of the reptation model.<sup>1,2</sup> The underlying assumption of reptation, that the obstacles provided by surrounding chains constrain a given chain to diffuse and relax stress by moving primarily along its own contour, has an appealing physical simplicity. On the basis of this assumption, it has proven possible to develop a suite of explicit predictions for dynamic observables as functions of the relevant molecular variables, and overall the agreement between experiment and theory has been very encouraging.<sup>3</sup> This agreement is often greatly enhanced by including one or both of two modifications to the bare reptation model: constraint release (CR) and contour length fluctuations (CLF). The former accounts for the mobility of the neighboring chains, which can release entanglements all along the contour of the test chain,<sup>4</sup> and the latter for the ability of the chain ends to explore some region of space without motion of the entire chain along its tube.<sup>5</sup> Despite this success, however, there have been some persistent discrepancies between the predictions of the model and the experimental results. Other nonreptative treatments,<sup>6–8</sup> most notably the polymer mode-coupling approach of Schweizer and co-workers,<sup>9–12</sup> can apparently resolve some or all of these issues, but it remains an interesting question as to whether the simpler reptation approach can do so too.

Foremost among these discrepancies is the observation that the zero shear viscosity,  $\eta$ , of entangled

solutions and melts scales as a power law in molecular weight,  $M$ , with an exponent of  $3.4 \pm 0.2$ ,<sup>13,14</sup> whereas the theory anticipates an exponent of 3.0. This difference was originally attributed to CLF by Doi,<sup>5</sup> and a recent analysis by Milner and McLeish provides a more quantitative demonstration that CLF can yield an exponent of 3.4 up to several hundred entanglements per chain, before crossing over to the asymptotic 3.0.<sup>15</sup> On the other hand, extensive measurements of melt self-diffusion coefficients,  $D$ , have been reported to be in excellent agreement with the predicted scaling  $D \sim M^{-2.0}$ .<sup>2,16</sup> Stronger apparent exponents, e.g., up to  $-2.5$ , have sometimes been discerned in the unentangled-to-entangled crossover regime and have been reconciled via incorporation of CR. Superficially, then, the behavior of  $\eta$  and  $D$  appears to be consistent with reptation, when modified by CR and CLF. However, there are several further difficulties to be addressed. First, measurements of  $D$  in well-entangled solutions uniformly obtain molecular weight exponents stronger than  $-2.0$ , typically in the vicinity of  $-2.4$  or  $-2.5$ , whereas the corresponding viscosity exponent remains 3.4.<sup>17–21</sup> In one study the diffusion exponent of  $-2.5$  persisted to almost 100 entanglements per chain,<sup>19</sup> and in another the exponent was approximately  $-2.7$  in a gel matrix;<sup>22</sup> neither observation is consistent with an explanation based on CR. These data, therefore, raise the possibility that the dynamics in entangled solutions differ in some fundamental way from those in melts, a difference not anticipated by reptation models. Second, the melt results imply that the longest chain relaxation time extracted from viscosity or stress relaxation has a different  $M$  dependence than the longest relaxation time

\* Author for correspondence. E-mail lodge@chem.umn.edu.

implied by  $D$ ,<sup>23,24</sup> whereas the model equates both times with the time to escape completely from the tube.<sup>2</sup> Although it has been argued in the past that CLF should not affect the  $M$  scaling of  $D$ ,<sup>5,24</sup> this view conflicts with some simulations<sup>25,26</sup> and a more recent treatment based on the Milner–McLeish version of CLF.<sup>27</sup> Third, tracer diffusion measurements have shown clearly that the diffusion exponent depends on matrix molecular weight,<sup>17,28–31</sup> which is not consistent with explanations based solely on CLF. A self-consistent treatment incorporating both CR and CLF is necessary.

Of the above issues, the really puzzling anomaly is the concentration dependence of the diffusion exponent; why does it change from ca.  $-2.5$  in solutions to  $-2.0$  in melts? In an attempt to shed some light on this, we undertook an extensive study of both  $D$  and  $\eta$  in concentrated hydrogenated polybutadiene (hPB) solutions. This system was selected on the basis of a very low entanglement molecular weight ( $M_e = 950$  g/mol in the melt), to achieve highly entangled chains even in moderately concentrated solutions, and a low glass transition temperature, to minimize any concentration dependence of the monomeric friction factor. There are also extensive melt data on this system in the literature,<sup>32–36</sup> which can serve as a reference. We report here on the detailed concentration (polymer volume fractions  $\phi$  from 0.2 to 1) and molecular weight dependences ( $4900 \leq M \leq 440\,000$  g/mol) of  $D$  and  $\eta$ . In particular, these data represent the first extensive measurements of  $D$  for highly concentrated solutions ( $\phi > 0.4$ ). The results are compared with other data in the literature and with the predictions of various models including, but by no means exclusively, those based on reptation. In a previous report we described the concentration dependence of the correlation length and entanglement spacing in these solutions.<sup>37</sup>

The main conclusion of this work is that the self-diffusion coefficient of entangled polymer liquids scales with a molecular weight exponent in the range  $-2.2$  to  $-2.5$ , both in solution and in the melt. As we recently demonstrated,<sup>38</sup> this is true for previous measurements of hPB in the melt,<sup>32–36</sup> despite the prevalent impression that  $D \sim M^{-2.0}$ .<sup>2,16</sup> We further demonstrate that  $D \sim M^{-2.3}$  provides a reasonable description for all other melt systems examined extensively in the literature, including polystyrene,<sup>28–30,39–41</sup> poly(methylstyrene),<sup>30</sup> polybutadiene,<sup>42</sup> poly(ethylene oxide),<sup>43</sup> poly(dimethylsiloxane),<sup>43</sup> and polyisoprene.<sup>42</sup> This conclusion largely eliminates the anomaly that the longest relaxation times implied by  $D$  and  $\eta$  have different  $M$  dependences and either reduces or eliminates the need to invoke different dynamic mechanisms in solutions and melts.

## Experimental Section

**Samples and Solutions.** Eight polybutadienes (PB) were prepared by living anionic polymerization of 1,3-butadiene in cyclohexane at 40 °C, using *sec*-butyllithium as the initiator. Portions of each polymer were then hydrogenated (or deuterated) in a high-pressure reactor using Pd/CaCO<sub>3</sub> as the catalyst. The molecular weights and polydispersities were determined by size exclusion chromatography in four different modes. The PB precursors were examined against a calibration based on PB standards and also utilizing a multiangle laser light scattering detector (Wyatt DAWN) to ascertain the molecular weights directly. The hydrogenated (deuterated) polymers h(d)PB were also run on a high-temperature chromatograph (Waters 150C), and the molecular weights were determined by universal calibration against polystyrene standards. These three methods gave consistent results, with

**Table 1. Molecular Weight Characterization of h(d)PB Samples**

polymer	$M_w$ , "A" <sup>a</sup>	$M_w$ , "B" <sup>b</sup>	$M_w$ , ave	$M_w/M_n$ <sup>c</sup>
hPB-5	4.8	5.0	4.9	1.01
hPB-10	10	10.7	10.3	1.002
hPB-20	23	23.6	23.3	1.002
hPB-50	51	55.4	53.2	1.003
hPB-100	110	96.6	103	1.02
dPB-100	110	112	111	1.01
hPB-200	180	208	194	1.01
dPB-200	190	215	203	1.01
hPB-350	360	340	350	1.03
dPB-350	370	357	364	1.03
hPB-420	460	361	410	1.17
dPB-420	480	410	440	1.04

<sup>a</sup> Average of three different SEC determinations, as described in the text. Molecular weights in kilodaltons. <sup>b</sup> Molecular weights from high-temperature SEC with light scattering detection on the saturated materials. <sup>c</sup> Polydispersities from high-temperature SEC with light scattering detection.

somewhat increased variation at higher molecular weight; the results were averaged and designated "set A" (see Table 1). Subsequently, the h(d)PB were run on a high-temperature chromatograph (Polymer Labs 210) at DuPont Central Research and Development, and the molecular weights were determined by a multiangle laser light scattering detector (Wyatt DAWN). The solvent was trichlorobenzene, the temperature was 135 °C, and  $dn/dc$  was set equal to  $-0.100$  g/mL. Although  $dn/dc$  might exhibit a slight dependence on  $M$  at low  $M$  and on deuteration, the uncertainties in determining each  $dn/dc$  would almost certainly be larger than the error introduced by assuming a common value. The resulting values of  $M$  are designated "set B" and are also listed in Table 1. "Set A" and "set B" are in very good agreement, to within 10% or better for all but the highest  $M$  sample. Accordingly, we employ the average of the two sets as the appropriate values of  $M_w$ . This approach emphasizes the high-temperature light scattering measurements, on the assumption that an absolute molecular weight method applied to the actual polymers to be studied is preferable. The polydispersities listed in Table 1 are taken from the "set B" measurements, because the light scattering detector is less influenced by band broadening. With the exception of hPB-420 (where the number denotes the approximate  $M$  in kg/mol), the distributions are suitably narrow. This polymer was therefore not used for rheology or as the tracer in diffusion measurements.

The microstructure of the PB and the degree of saturation of the h(d)PB were assessed by <sup>1</sup>H NMR. The former ranged from 7.3% 1,2-addition for PB-50 to 4.2% for PB-420, and the latter was consistently greater than 99%. Consequently, these polymers may be viewed as random copolymers of ethylene and 1-butene, with from 1.9 to 1.1 ethyl branches per 100 backbone carbons; they would be designated PEB-2 or PEB-1 in the nomenclature employed elsewhere.<sup>44</sup> A Perkin-Elmer DSC-7 was used to measure the melting temperature,  $T_m$ , and the percent crystallinity in each sample following standard procedures. Table 2 lists the microstructure,  $T_m$ , and percent crystallinity for these polymers. The partial deuteration systematically lowers  $T_m$  by 1–3 °C, consistent with previous reports.<sup>33</sup> On the basis of a density gradient column method applied at room temperature,<sup>45</sup> we estimate the fractional deuteration to be 0.44 for dPB-350 and dPB-420. Linear alkane solvents were obtained from Aldrich (C<sub>24</sub>H<sub>50</sub>) and CDN Isotopes (C<sub>16</sub>D<sub>34</sub>). Solutions were prepared gravimetrically, using toluene as a cosolvent, and annealing above the melting temperature of hPB (110–120 °C). A small quantity (<0.5%) of antioxidant (BHT) was added to each sample. Concentrations are reported as volume fraction polymer,  $\phi$ , calculated assuming additivity of volumes and densities at 140 °C of 0.782<sub>g</sub>, 0.724<sub>g</sub>, and 0.795<sub>g</sub> mL for hPB,<sup>45</sup> C<sub>24</sub>H<sub>50</sub>, and C<sub>16</sub>D<sub>34</sub>,<sup>46</sup> respectively.

**Rheology.** Measurements of the dynamic shear moduli,  $G'$  and  $G''$ , were performed on a Rheometric Scientific DSR in

**Table 2. Microstructure and Crystallinity of h(d)PB Samples**

polymer	% 1,2	$T_m$ , °C	% cryst
hPB-5	6.5	115.5	45
hPB-10	6.5	115.3	42
hPB-20	7.4	112.3	36
hPB-50	7.3	112.2	33
hPB-100	6.6	107.9	22
dpB-100	6.6	106.6	26
hPB-200	7.6	116.8	23
dpB-200	7.6	113.6	27
hPB-350	4.5	114.3	28
dpB-350	4.5	112.3	25
hPB-420	4.2	112.1	25
dpB-420	4.2	110.8	26

the parallel plate geometry. An 8 mm diameter plate with a serrated surface was employed as the top plate to reduce sample slip. The bottom plate was a 25 mm plate with a smooth surface. The typical gap thickness was 0.8–1.3 mm. Strain amplitudes of 0.03–0.08 were sufficiently small to ensure linear response. The viscosities were determined from the low-frequency limiting behavior of  $G'$ . The measurements were corrected for the error in the torque measurement due to sample protrusion from the gap, following standard procedures.<sup>47</sup> Solutions of hPB-10, hPB-20, hPB-50, hPB-100, h(d)PB-200, h(d)PB-350, and dPB-420, with concentrations ranging from  $\phi = 0.05$  to 1.0, were examined. The longer  $n$ -alkane was used for the rheological measurements, to minimize solvent evaporation at elevated temperatures. It is assumed that the presence of deuterium has no effect on the dynamic moduli. For each solution measurements were taken at several temperatures, including  $140 \pm 1$  °C. A minimum of four temperatures were examined for each solution (typically 120, 130, 140, and 150 °C), but in some cases as many as eight temperatures (from 110 to 190 °C) were used. This permitted determination of the activation energy for the viscosity,  $E_\eta$ , as a function of  $M$  and  $\phi$ . The viscosity of dPB-420 was also remeasured on a Rheometric Scientific ARES instrument, with 7.92 mm diameter plates and an 0.5 mm gap; the results were identical to those obtained on the DSR.

**PFG-NMR.** The PFG-NMR measurements were performed at the University of Akron. The experimental technique has been described in detail,<sup>48–50</sup> and therefore only a brief review is given here. A pulse gradient of duration  $\delta$  and magnitude  $G$  is applied during a  $90^\circ - \tau_1 - 90^\circ - \tau_2 - 90^\circ$  radio-frequency (rf) pulse sequence. Under these conditions, the spin echo is attenuated by spin–spin relaxation as well as molecular diffusion. The gradient  $G$  was typically on the order of 186 G/cm. The separations between the first and second rf pulse, and between the first and third, were 21 and 150 ms, respectively. The gradient pulses were applied 0.1 ms after the first and after the third rf pulses, with a separation,  $\Delta$ , of 150 ms. The ratio of the echo height with and without the field gradient pulses is given by

$$R = 0.5 \exp \left[ A - (\gamma G \delta)^2 D \left( \Delta - \frac{\delta}{3} \right) \right] \quad (1)$$

where  $A$  is a cluster of parameters that are related to the spin–spin relaxation time and the separation between the second and third rf pulses, and  $\gamma = 2.68 \times 10^4$  rad/(s G) is the proton gyromagnetic ratio. The value of  $D$  is obtained from the slope of a plot of  $\ln R$  versus  $(\gamma G \delta)^2 (\Delta - \delta/3)$ . Solutions for PFG-NMR measurements were prepared in  $C_{16}D_{34}$ . Measurements were taken on hPB-5, hPB-10, hPB-20, hPB-50, and dpB-100 for  $\phi = 0.2$ . The sample temperature was controlled to  $140.5 \pm 0.5$  °C, and for the solutions of hPB-10, hPB-20, and hPB-50 with  $\phi = 0.20$  measurements were repeated at several temperatures from 120.5 to 200.5 °C, to permit determination of the diffusional activation energy,  $E_D$ .

**Forward Recoil Spectrometry** The principles of the FRES technique can be found in many references<sup>51,52</sup> and are not repeated here. A 3 MeV  $^4\text{He}^{2+}$  beam impinging on a bilayer sample at an angle of  $15^\circ$ . The forward recoiling protons and

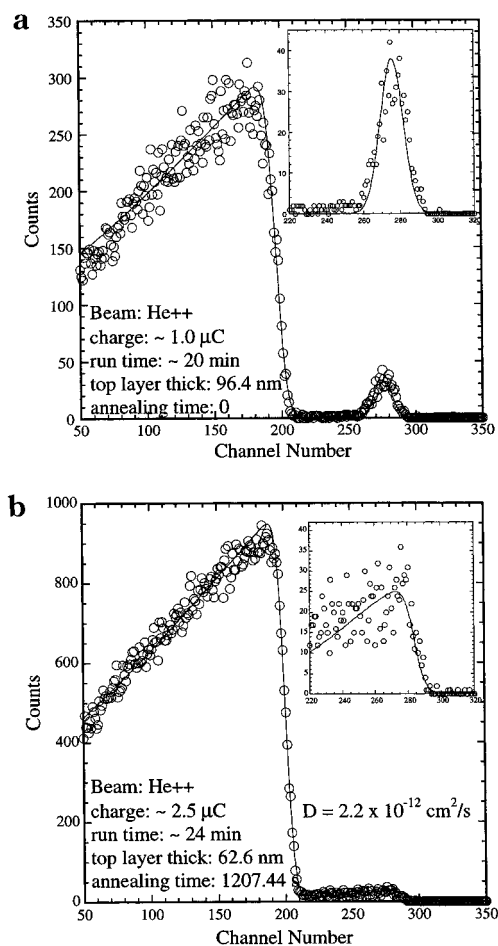


**Figure 1.** FRES spectrum for (a) an unannealed d(h)PB-420 couple,  $\phi = 0.769$  in  $C_{24}H_{50}$ , and (b) the same couple after annealing.

deuterons were detected at a takeoff angle of  $15^\circ$  after passing through a  $12 \mu\text{m}$  Mylar foil. To reduce the ion beam damage, the sample was cooled by constantly flowing liquid nitrogen underneath the sample, by reducing the beam intensity to ca. 2 nA, and by moving the beam to a different sample spot after taking a spectrum for ca. 2 min. The resulting “master” spectrum was the sum of approximately 20 smaller spectra. Parts a and b of Figure 1 show typical FRES spectra of unannealed and annealed h(d)PB-420 in  $C_{24}H_{50}$  ( $\phi = 0.769$ ), respectively. The spectra are fit with the standard software routine RUMP, with the diffusivity the only adjustable parameter.

FRES samples were prepared as follows. A thick bottom layer ( $> 1 \mu\text{m}$ ) of hPB/ $C_{24}H_{50}$  was cast onto a silicon wafer from hot toluene solution (ca. 100 °C). A thin top layer (50–100 nm) is then produced by spin-casting a hot dpB/ $C_{24}H_{50}$  toluene solution (ca. 100 °C) onto a freshly peeled mica surface. The top layer is floated off the mica onto the surface of a distilled water bath and picked up on the hPB/ $C_{24}H_{50}$ -coated wafer. The bilayer sample is then annealed in an air oven at 140 °C to allow diffusion to take place before the FRES measurement. The top layer is thicker than the ca. 20 nm films typically used for FRES diffusion measurements, although it is comparable to the layers employed by Crist et al.<sup>34</sup> As dpB is only partially deuterated, and further diluted by solvent, a thicker top layer is desirable to increase the signal. As the top and bottom layers are chemically equivalent except for the isotopic labeling, the thicker top layer should not affect the measured depth profile.

## Results

The presentation of the results is organized as follows. First we consider the temperature dependence of  $\eta$  and



$D$ , to assess whether the monomeric friction factor exhibits any significant dependence on  $\phi$  or  $M$ . Second, we examine the  $\phi$  and  $M$  dependence of  $\eta$  and, third, the  $\phi$  and  $M$  dependence of  $D$ . Further analysis of the results, and comparisons with other data in the literature, are deferred to the Discussion section.

**Temperature Dependence.** It is generally accepted that any chain dynamics property of a polymer liquid can be factored into the product of two functions: one that depends on the mechanism of motion (such as reptation) and the other on the time scale for segmental rearrangements.<sup>13,14</sup> The former depends on  $\phi$  and  $M$  but not on  $T$ , and the latter depends on  $T$  (or  $T - T_g$ ) but not  $M$ . For example, the Rouse and reptation model predictions for the self-diffusion coefficient of a linear homopolymer in the melt may be written as follows:

$$D_{\text{Rouse}} = \frac{kT}{N\zeta}; \quad D_{\text{rep}} = \frac{M_e}{M} D_{\text{Rouse}} \quad (2)$$

where  $\zeta$  is the monomeric friction factor and  $N$  is the degree of polymerization.<sup>2</sup> In both cases the "second function" is  $kT/\zeta$ , where  $\zeta(T)$  is characteristic of a given polymer structure. The experimental  $\phi$  dependence in solution is often complicated by the unknown  $\phi$  dependence of  $\zeta$ , but it is generally assumed that the  $\phi$  dependence enters primarily through  $T_g$ . Typically  $T_g$  increases with  $\phi$ , and thus  $\zeta$  develops a stronger  $T$  dependence as  $\phi$  increases. However, it is certainly possible that  $\zeta$  could have an additional composition dependence even if  $T_g$  were independent of  $\phi$ .

As noted in the Experimental Section, we examined the  $T$  dependence of both  $\eta$  and  $D$  for all of the solutions. As representative examples, the results are shown in Figure 2a,b for solutions of hPB-20 with  $\phi > 0.18$ . Both quantities are plotted logarithmically versus  $1/T$ , to illustrate that the Arrhenius dependence is followed. The activation energies are therefore extracted as

$$E_\eta \equiv -R \frac{d \ln \eta}{d(1/T)}; \quad E_D \equiv -R \frac{d \ln D}{d(1/T)} \quad (3)$$

The values of  $E_\eta$  and  $E_D$  are listed in Table 3 and plotted in Figure 3 as a function of  $\phi M$ ; this choice of independent variable is intended solely to spread the data out. Although the data are scattered, due primarily to the limited range of  $T$  involved, overall it is clear that there is no significant dependence on either  $\phi$  or  $M$ . We thus conclude that there is no  $M$  dependence to  $\zeta$  in our measurements, and therefore no "free volume" correction is needed. The possibility remains that there is a weak  $\phi$  dependence to  $\zeta$  that is not reflected in a change in  $T$  dependence.

The  $M$  independence is consistent with the results of Pearson et al., who found that  $\zeta$  in the melt is independent of  $M$  above  $M \approx 3000$  g/mol.<sup>53</sup> The average value of  $E_\eta$  is 27.4 kJ/mol (std dev 3.8) and 28.9 kJ/mol (std dev 1.7) for the melt data alone. This compares favorably with the reported value of 30 (std dev 1) for hPB melts by Raju et al.<sup>54</sup> Pearson et al. investigated the  $T$  dependence in more detail for PE and hPB melts, utilizing the Vogel equation.<sup>36</sup> The observed deviation from an Arrhenius dependence is not substantial over the temperature range considered here, and their results for high  $M$  correspond to  $E_\eta = 28$  kJ/mol at 140 °C. Our average value of  $E_D$  is 27.3 kJ/mol (std dev 2.9), in good agreement with the value of 26 kJ/mol reported by Bartels et al.<sup>33</sup> Our values of  $E_\eta$  and  $E_D$  are identical

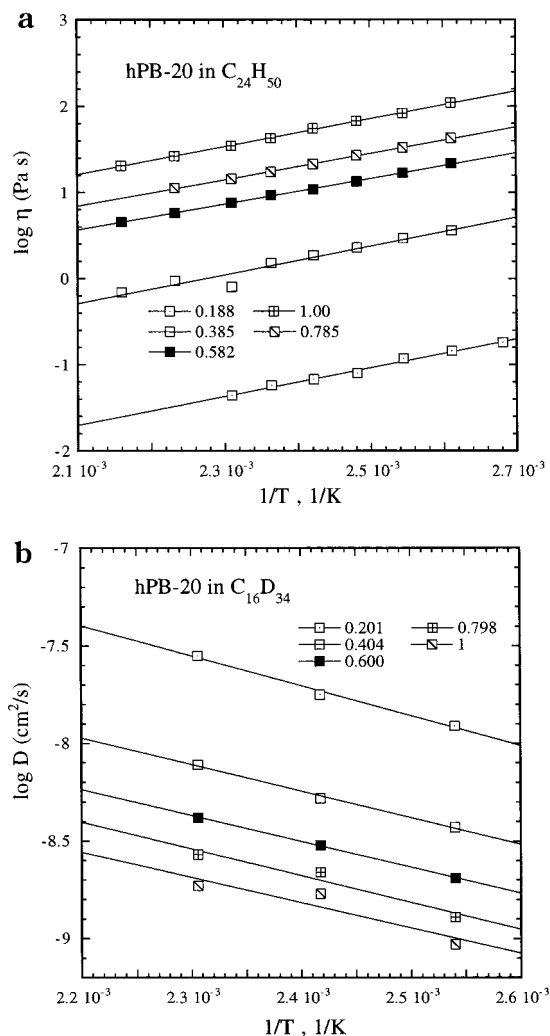


**Figure 2.** Temperature dependence of (a) viscosity and (b) diffusion for hPB-20 solutions.

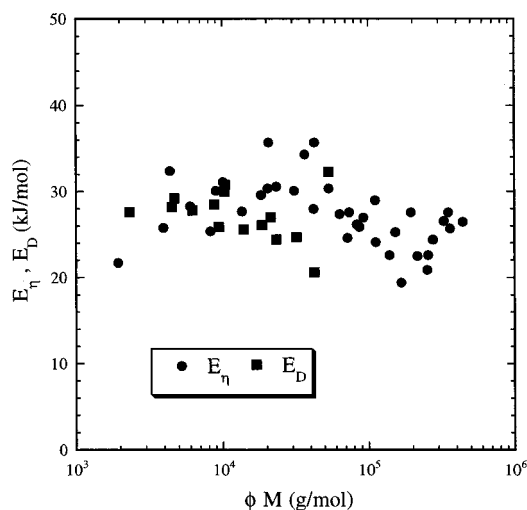
within the experimental uncertainty, which is in apparent conflict with the conclusion of Bartels et al., that  $E_\eta - E_D \approx 4$  kJ/mol.<sup>33</sup> (In the reptation model this difference arises from the way in which the  $T$  dependence of the chain dimensions and density enter  $D$  and  $\eta$ .) However, our activation energy data are actually not sufficiently precise to draw any conclusions on this point.

**Viscosity.** The measured viscosities are reported in Table 4; these values represent interpolations of the data obtained at four or more temperatures, as described in the Experimental Section. The melt data are plotted as a function of  $M$  in Figure 4, along with results from the literature. The latter were tabulated for 175 °C by Pearson et al.,<sup>36</sup> having been collated from various sources,<sup>33–35</sup> and we have adjusted them to 140 °C. The temperature shift factor utilized is 1.82, which represents a compromise between 1.87 implied by our value of  $E_\eta$  and 1.76 based on the Vogel dependence reported by Pearson et al.<sup>36</sup> The literature data have been fit to a power law, with the resulting exponent being 3.43. With the possible exception of dPB-420, our data are in excellent agreement with the previous workers.

All of the data in Table 4 are plotted in Figure 5, as a function of  $M/M_e$ . The concentration dependence of  $M_e$  was determined previously,<sup>37</sup> and combining our measurements with those of Raju et al. for hPB in paraffin

**Table 3. Activation Energies for Viscosity and Diffusion**

polymer	$\phi$	$E_\eta$		$\phi$	$E_D$	
		kJ/mol	$\Delta E_\eta$		kJ/mol	$\Delta E_D$
hPB-10	0.187	21.7	0.1	0.225	27.6	3.1
	0.382	25.8	0.1	0.439	28.2	2.2
	0.580	28.3	0.1	0.603	27.8	1.6
	0.796	25.4	0.4	0.850	28.5	1.0
hPB-20	1.000	30.8	0.5	1.000	30.0	8.7
	0.188	32.4	4.6	0.201	29.2	0.5
	0.385	30.1	0.6	0.404	25.9	5.7
	0.581	27.7	0.7	0.600	25.6	0.6
hPB-50	0.785	29.6	0.3	0.798	26.1	1.9
	1.000	30.6	1.6	1.000	24.4	2.8
	0.189	31.1	0.5	0.195	30.8	2.9
	0.382	30.4	1.4	0.401	27.0	0.3
hPB-100	0.578	30.1	0.3	0.599	24.7	1.5
	0.787	28.0	0.3	0.798	20.6	5.3
	1.000	30.4	0.2	1.000	32.3	2.2
hPB-200	0.185	35.7	3.2			
	0.382	35.7	0.3			
	0.570	27.4	1.6			
	0.780	25.9	2.0			
hPB-350	1.000	29.0	0.5			
	0.187	34.3	0.6			
	0.381	27.6	0.5			
	0.476	27.0	0.1			
dPB-100	0.578	24.1	0.3			
	0.786	25.3	0.1			
	1.000	27.6	0.5			
	0.205	24.6	0.3			
dPB-200	0.397	22.6	0.7			
	0.613	22.5	0.3			
	0.717	20.9	0.7			
	0.785	24.4	0.5			
dPB-420	0.933	26.6	0.4			
	1.000	27.6	0.4			
	0.189	26.2	0.7			
	0.379	19.4	0.9			
dPB-420	0.580	22.6	0.5			
	0.817	25.7	0.2			
	1.000	26.5	0.9			

**Figure 3.** Activation energies for viscosity and diffusion for various concentrations and molecular weights.

waxes,<sup>55</sup> we obtain the simple result that  $M_e \approx 950/\phi$  g/mol. Consequently, Figure 5 is equivalent to a plot of  $\eta$  versus  $\phi M$ ; the latter has been used in the past as a reducing variable for solution viscosities.<sup>13,14</sup> The data in Figure 5 reduce to a reasonable master curve, albeit not perfectly. The implication is that in this system  $\eta$  depends primarily on the number of entanglements per chain, in both solutions and melts. In an attempt to explore whether there is an additional  $\phi$  dependence, the data were examined as a function of  $(\phi M)\phi^x$ , where

$x$  is small. A slightly better superposition was obtained for  $x = 0.15$  (not shown). If we take this result at face value, the additional  $\phi$  dependence could be easily attributed to at least two sources. One could be  $\zeta$ , and another could be uncertainty in the  $\phi$  dependence of  $M_e$ . Although our results gave  $G_N \sim \phi^{1.9}$ <sup>37</sup> (where  $G_N$  is the plateau modulus), Raju et al. obtained  $G_N \sim \phi^{2.2}$ ,<sup>55</sup> which would imply  $M_e \sim \phi^{1.2}$ . The precision of the data precludes drawing a firm conclusion on this point, but the dominant role of  $M/M_e$  in determining  $\eta$  is apparent.

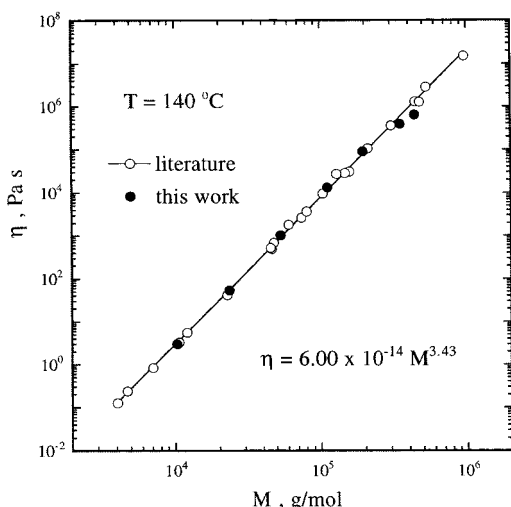
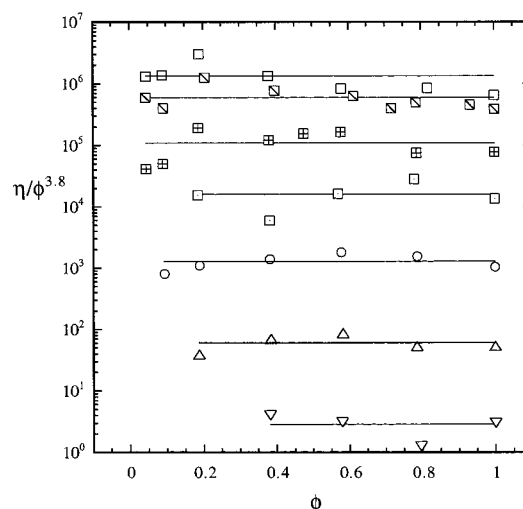
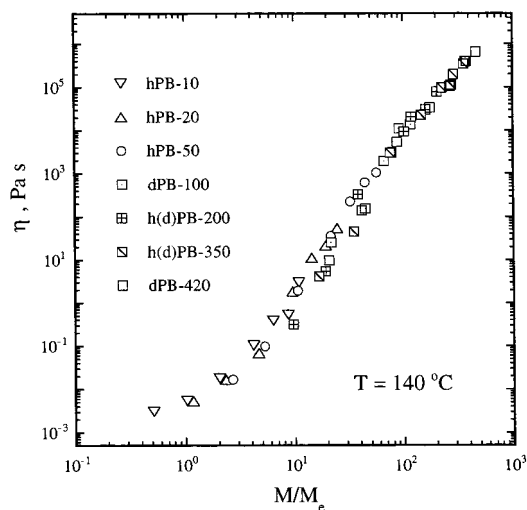
To explore the  $\phi$  dependence of  $\eta$  explicitly, we examined  $\eta$  versus  $\phi$ , restricting attention to those solutions for which  $M/M_e > 3$  (following the general result that the crossover to entangled behavior in the viscosity occurs at an  $M_e \approx 2-3M_e$ ).<sup>14</sup> Fits to a power law for each  $M$  were reasonable and gave exponents in the range 3.6–4. However, given the scatter in the data and the limited number of concentrations for a given  $M$ , it is plausible to describe all of the data with a common exponent. To illustrate this, we plot  $\eta/\phi^{3.8}$  versus  $\phi$  in Figure 6, where the average value for each  $M$  is shown as a horizontal line. The deviations about each horizontal line show no obvious correlation with  $\phi$ , and accordingly we conclude that  $\eta$  is reasonably well described as a power law in  $\phi$ , with an exponent of  $3.8 \pm 0.2$ . Such an exponent is consistent with several previous studies.<sup>56,57</sup> The average values of  $\eta/\phi^{3.8}$  from Figure 6 are plotted versus  $M$  in Figure 7, with the resulting exponent being 3.46. Clearly the exact value of this exponent would depend on the  $\phi$  exponent selected, but the important result is that the  $M$  dependence of  $\eta$  for these solutions is (a) consistent with the literature and (b) not a function of  $\phi$  when  $M/M_e > 3$ . Of course, it is possible to fit  $\eta$  versus  $M$  for each  $\phi$  (although some interpolation of the data is necessary to make each  $\phi$  the same), and the resulting power laws (not shown) give exponents from 3.3 to 3.5. Thus, we may conclude that for these solutions  $\eta$  scales as  $M^{3.4 \pm 0.1} \phi^{3.8 \pm 0.2}$ .

**Diffusion.** The diffusion data are listed in Table 5. The FRES data for dPB-350 and dPB-420 only extend down to  $\phi \approx 0.6$ , due to the weak signals (see Figure 1). The NMR data for the dPB-100 and hPB-50 melts, and for dPB-100 with  $\phi \approx 0.8$ , were also discarded as being unreliable due to the low values of  $D$ . The remaining data were fit to power laws, as with  $\eta$ . Each power law is a good representation of the data, but again the resulting exponents (which are scattered about  $-1.8$ ) should not be granted too much significance, due to the small range of  $\phi$  and the small number of points involved. Indeed, it is reasonable to postulate that a single power law exponent applies to all  $M$ ; thus, in analogy to Figure 6, in Figure 8 we plot  $D\phi^{1.8}$  versus  $\phi$ , where 1.8 was chosen as representative of the individual values. The horizontal lines in Figure 8 denote the average values obtained, and this plotting format demonstrates that to a good approximation  $D \sim \phi^{-1.8}$ . The average values themselves are plotted against  $M$  in Figure 9 and when fit to a power law give an exponent of  $-2.41$ . This approach assumes that the  $M$  exponent is independent of  $\phi$ , which is necessarily only as good an assumption as that a single  $\phi$  exponent describes all the different  $M$  data sets. To examine the  $M$  dependence more directly, we took the power law fits to  $D(\phi)$  for each  $M$  and interpolated to  $\phi = 0.2, 0.4, 0.6$ , and  $0.8$ . The resulting values of  $D$  are plotted against  $M$  in Figure 10, and the power law exponents  $\alpha$  are

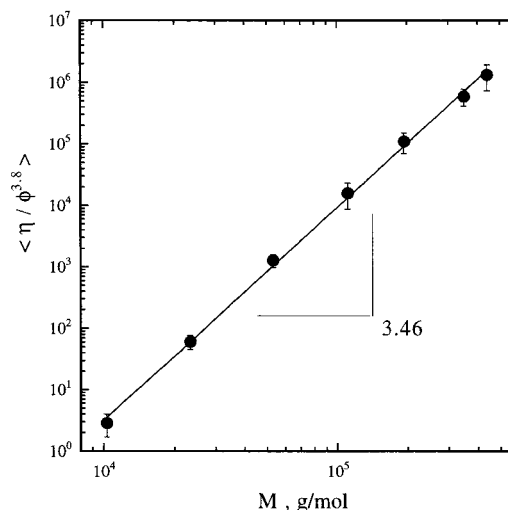
**Table 4. Viscosities of h(d)PB Solutions and Melts at 140 °C**

polymer	$M_w$ , kDa	$\log \eta$ , Pa.s						
		$\phi = 1.0$	0.8 <sup>a</sup>	0.6 <sup>a</sup>	0.4 <sup>a</sup>	0.2 <sup>a</sup>	0.1 <sup>a</sup>	0.05 <sup>a</sup>
hPB-10	10.3	0.48	-0.27 (0.796)	-0.41 (0.580)	-0.98 (0.382)	-1.74 (0.187)	-2.26 (0.095)	-2.51 (0.047)
hPB-20	23.3	1.73	1.33 (0.785)	1.05 (0.581)	0.27 (0.385)	-1.17 (0.188)	-1.77 (0.094)	-2.27 (0.048)
hPB-50	53.2	3.02	2.80 (0.787)	2.35 (0.578)	1.56 (0.382)	0.29 (0.189)	-1.00 (0.093)	-1.77 (0.047)
dPB-100	111	4.13	4.04 (0.780)	3.26 (0.570)	2.19 (0.382)	1.40 (0.185)		
hPB-200	194	4.96	4.48 (0.786)	4.31 (0.578)	3.49 (0.381)	2.51 (0.187)		
dPB-200	203				3.97 <sup>b</sup> (0.476)		0.73 (0.090)	-0.50 (0.045)
hPB-350	350	5.60	5.29 (0.785)	4.99 (0.613)	4.36 (0.397)	3.48 (0.205)		
dPB-350	364		5.54 <sup>b</sup> (0.933)	5.05 <sup>b</sup> (0.717)			1.65 (0.091)	0.61 (0.044)
dPB-420	440	5.81	5.59 (0.817)	5.02 (0.580)	4.52 (0.379)	3.73 (0.189)	2.14 (0.089)	0.99 (0.045)

<sup>a</sup> Nominal solution volume fraction; actual value in parentheses. <sup>b</sup> Note that volume fractions are far from the nominal value.

**Figure 4.** Melt viscosity for hPB from this work and from the literature.**Figure 6.** Viscosity normalized by  $\phi^{3.8}$  versus concentration. Samples from top to bottom: dPB-420, h(d)PB-350, h(d)PB-200, dPB-100, hPB-50, hPB-20, and hPB-10.**Figure 5.** Viscosity of hPB melts and solutions versus the number of entanglements per chain.

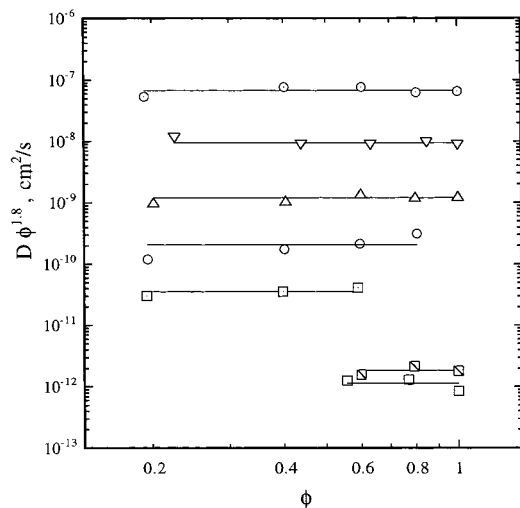
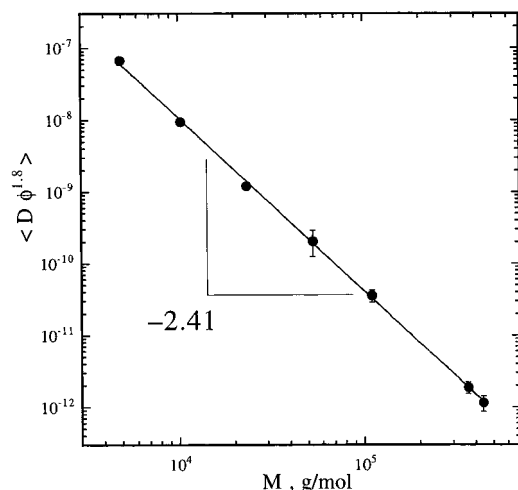
indicated on the plot. The values range from -2.4 to -2.5, and the indicated uncertainties correspond to a 95% confidence interval. Thus, overall we conclude that our data are consistent with  $D \sim M^{-2.4 \pm 0.1} \phi^{-1.8 \pm 0.2}$ .

**Figure 7.** Average values of  $\eta/\phi^{3.8}$  from Figure 7 versus molecular weight.

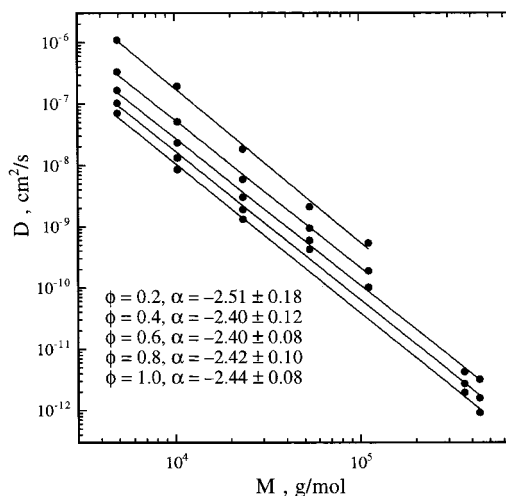
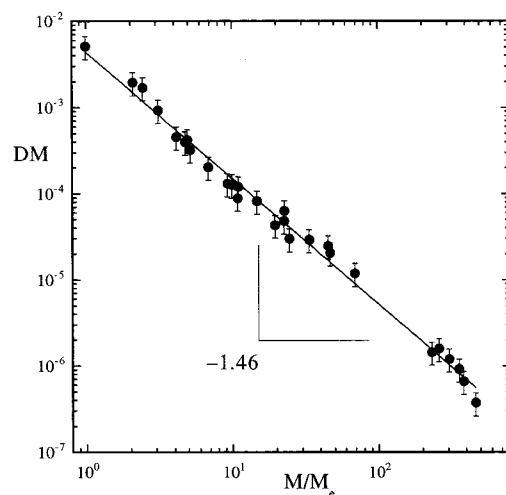
The data may also be examined as a function of the number of entanglements per chain,  $M/M_e$ . Equation 2 suggests that the appropriate way to do this is by

**Table 5. Diffusivities of h(d)PB Solutions and Melts at 140 °C**

polymer	$M_w$ , kDa	$\phi = 1.0$	log $D$ , cm <sup>2</sup> /s			
			0.8 <sup>a</sup>	0.6 <sup>a</sup>	0.4 <sup>a</sup>	0.2 <sup>a</sup>
hPB-5	4.9	-7.18	-7.03 (0.804)	-6.72 (0.603)	-6.40 (0.402)	-5.98 (0.192)
hPB-10	10.3	-8.06	-7.89 (0.850)	-7.70 (0.603)	-7.41 (0.439)	-6.78 (0.225)
hPB-20	23.3	-8.89	-8.73 (0.798)	-8.45 (0.600)	-8.26 (0.404)	-7.74 (0.201)
hPB-50	53.2		-9.35 (0.798)	-9.27 (0.599)	-9.00 (0.401)	-8.57 (0.195)
dPB-100	111			-9.95 (0.590)	-9.73 (0.398)	-9.20 (0.194)
dPB-350	364	-11.74	-11.48 (0.792)	-11.40 (0.581)		
dPB-420	440	-12.07	-11.68 (0.769)	-11.44 (0.557)		

<sup>a</sup> Nominal solution volume fraction; actual value in parentheses.**Figure 8.** Diffusivity normalized by  $\phi^{-1.8}$  versus concentration. Samples from top to bottom: hPB-5, hPB-10, hPB-20, hPB-50, dPB-100, dPB-350, and dPB-420.**Figure 9.** Average values of  $D\phi^{1.8}$  from Figure 9 versus molecular weight.

plotting  $DM$  against  $M/M_e$ , where the factor of  $M$  represents the Rouse diffusivity. Accordingly, the data are plotted in this format in Figure 11. The data reduce reasonably well to a master curve, with an unfortunate but unavoidable lacuna between the NMR and FRES data sets. A global fit to a power law gives a slope of  $-1.46$ , implying an  $M$  exponent of  $-2.46$ . In the case of

**Figure 10.** Diffusivities, interpolated to the precise concentrations, versus molecular weight.**Figure 11.** Product of diffusivity and molecular weight for hPB solutions versus the number of entanglements per chain.

the viscosity, a slightly different  $\phi$  dependence was also explored, and accordingly we tried the corresponding modification for the diffusion data; i.e., we changed the horizontal axis to  $(M/M_e)\phi^{0.15}$ . The reduction to a master curve was of comparable quality, and the implied exponent was essentially identical ( $-1.43$ ).

The crucial result from the diffusion data, of course, is that the  $M$  exponent is substantially stronger than the  $-2.0$  anticipated by reptation, both in concentrated solution and all the way up to the melt. These results will be compared with others in the literature in the ensuing discussion, but first it is important to examine the reliability of the data in more detail. From Figure 11 it is apparent that the strong exponents are heavily influenced by the FRES results. On the basis of the NMR data only, one might conclude that the data are approaching an exponent of  $-2.0$ ; indeed, we tentatively reached such a conclusion before the FRES data were incorporated.<sup>58</sup> The individual FRES  $D$  values represent the average of three or four different samples for each  $(\phi, M)$  pair, and the reproducibility was good (rel std dev from 4 to 40%). However, as is evident from Figure 1b, the signals are small and the data quite scattered about the fit. Thus, it is conceivable that there is a significant systematic error in  $D$ , particularly given the fact that these represent the first FRES measurements



from this laboratory. However, we may make a direct comparison with the measurement of  $D$  for a dPB with  $M = 424\,000$  at  $T = 125\text{ }^{\circ}\text{C}$  by Crist et al.<sup>34</sup> After correcting to  $140\text{ }^{\circ}\text{C}$  as with  $\eta$  above, their datum gives  $DM \approx 6.3 \times 10^{-7}$  for  $M/M_e = 447$ , which falls within 6% of the power law curve in Figure 11. Given this favorable comparison, and those to be made subsequently with measurements on hPB by other techniques, we conclude that there is no obvious reason to question the FRES results. The  $M$  exponent is also sensitive to the value of  $M$  at the extreme of the range, and one might therefore suspect dPB-420 in particular. However, the comparison with the  $\eta$  data from the literature suggests that, if anything, the actual  $M$  might be smaller than we determined, but if this were the case, the  $M$  dependence of  $D$  would increase, not decrease, so this seems improbable. We also note that the hPB-420 matrix was a little more polydisperse than the other samples, but as it is the matrix and not the tracer, this should have a rather negligible effect on  $D$ .

One further issue to consider is the possibility of "thermodynamic slowing down" in the FRES measurements (and also in the SANS<sup>33</sup> and infrared microdensitometry results<sup>35</sup>) due to the finite  $\chi$  parameter between hPB and dPB. The magnitude of the expected effect can be estimated by

$$\frac{D_{\text{exp}}}{D} = 1 - 2\phi_d(1 - \phi_d)\chi N \quad (4)$$

where  $D_{\text{exp}}$  is the measured mutual diffusion coefficient and  $\phi_d$  is the volume fraction of labeled chains,<sup>59</sup> utilizing experimental values for  $\chi$  (which depend on the extent of deuteration). However, quantitative application of eq 4 is inhibited by the fact that  $\phi_d$  is a function of both time and position within the sample. For example, in our FRES measurements  $\phi_d$  begins as 0, where there is no effect, and at very long times approaches ca. 0.1; in between there are regions in the sample where  $\phi_d$  exceeds 0.1. In the SANS experiments,  $\phi_d$  evolved from 0 to 0.5,<sup>33</sup> whereas in the infrared results  $\phi_d$  was always kept below 0.05.<sup>35</sup> The general agreement among these techniques suggests that the effect is not great, but the  $N$  dependence is potentially important. Taking the value of  $\chi$  given by Nicholson and Crist,<sup>60</sup> and utilizing  $\phi_d = 0.1$  as a "typical" situation and  $\phi_d = 0.5$  as a "worst case scenario", the predicted error in  $D$  would reach 30% by  $M/M_e \approx 500$  in the former case and by  $M/M_e \approx 200$  in the latter. Consequently, the effect is negligible for all but FRES results, where they may contribute to a reduction in  $D$  by as much as 30%; this is close to the estimated experimental uncertainty. Therefore, we conclude that there is no significant influence on the  $M$  exponents obtained so far for hPB melts, but there might be a tendency to mask a crossover to a weaker  $M$  dependence such as  $-2.0$  at the very highest  $M/M_e$ .

## Discussion

The discussion and further analysis of the data are divided into two parts. First, we will compare the results with those in the literature, particularly emphasizing the  $M$  dependence of  $D$ . Then we will compare the results with the predictions of various theoretical approaches.

**Comparison with Literature Diffusion Data.** As noted in the Introduction, measurements of  $D$  in well-

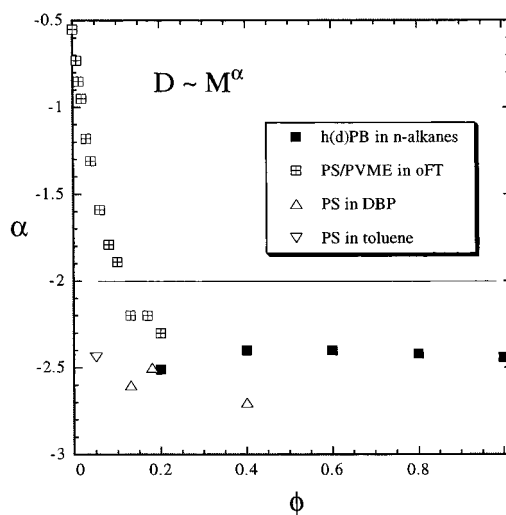


**Figure 12.** Molecular weight exponents,  $\alpha$ , for diffusion in entangled solutions from this work and from the literature.

entangled polymer solutions (i.e.,  $M/M_e > 5-10$ ) are rare but consistently give  $M$  exponents near  $-2.5$ .<sup>17,19-21</sup> This is illustrated in Figure 12, where the exponent  $\alpha$  is plotted against concentration for our data (from Figure 10) and for polystyrene (PS) in dibutyl phthalate (DBP)<sup>19,20</sup> and toluene.<sup>21</sup> The results for the different systems are in close agreement and taken together imply that this exponent is essentially independent of concentration once  $M/M_e$  is sufficiently large. The other set of exponents in Figure 12 come from previous work in this laboratory, where the tracer diffusion of PS was determined in high molecular weight poly(vinyl methyl ether) solution matrices.<sup>18</sup> We include these data to illustrate how the exponent changes smoothly from a value near  $-0.55$  at infinite dilution to values clearly stronger than  $-2.0$ . (Note that earlier reported exponents of  $-2.0$  were obtained from solutions in the unentangled-to-entangled crossover<sup>61,62</sup> and do not constitute direct evidence of reptation; rather, they are consistent with a point on the smooth progression illustrated in Figure 12.) The concentration at which the exponent achieves its apparent limiting value near  $-2.4$  or  $-2.5$  will depend on the range of  $M$  involved, and so the PS/PVME exponents in Figure 12 should not form a unique master curve with the other data sets.

Our data are compared directly with those of Nemoto et al. in Figure 13,<sup>19,20</sup> in the format of Figure 11 (i.e.,  $DM$  vs  $M/M_e$ ). Although the slopes extracted from best fits to a power law fluctuate among the four data sets shown, it is evident that they would superpose well upon the appropriate vertical shift. That the PS data for different concentrations do not superpose in this format, whereas the hPB data do, is a direct reflection of the nonnegligible  $\phi$  dependence of  $\zeta$  in the case of PS. Finally, we also note that other authors have measured  $D$  for PS in good solvent solutions in the vicinity of  $M/M_e \approx 1$ <sup>62-64</sup> and that Nemoto et al. have shown that these data may all be superposed by normalizing to  $D(M_e)$  (see Figure 11 of ref 20). Thus, overall we conclude that our solution data are generally consistent with those available for PS, with the obvious differences that our results (i) emphasize much higher concentrations and (ii) are not complicated by monomeric friction effects.

The comparison with self-diffusion data for melts is particularly provocative. Many different polymers have been examined over the past two decades, including



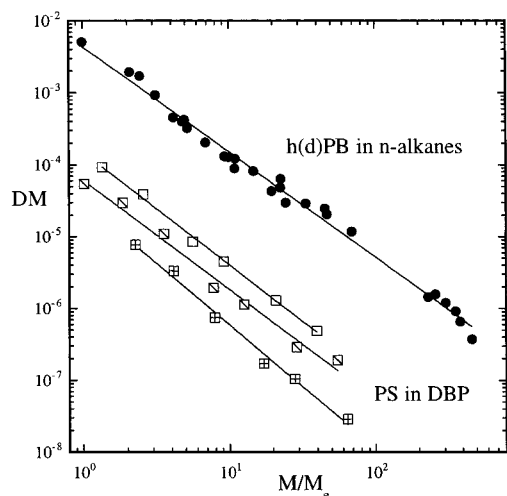


**Figure 13.** Product of diffusivity and molecular weight for hPB solutions (this work) and for polystyrene in dibutyl phthalate (literature) versus the number of entanglements per chain.

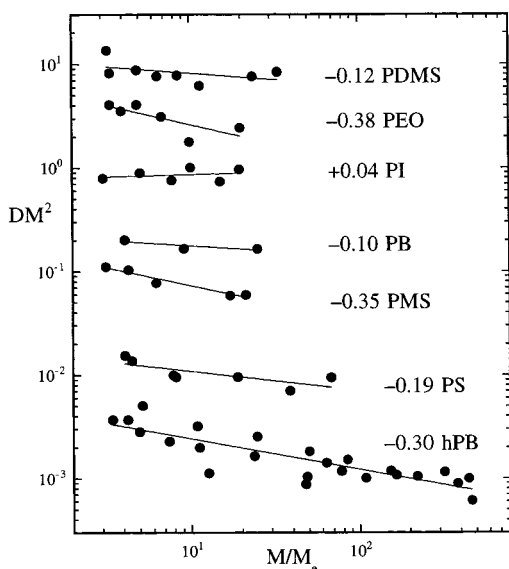


**Figure 14.** Product of melt diffusivity and molecular weight squared for seven different polymers, from the literature and from this work.

PS,<sup>28–30,39–41</sup> hPB,<sup>32–36</sup> polyethylene (PE),<sup>53,65–70</sup> polyisoprene (PI),<sup>42</sup> polybutadiene (PB),<sup>42</sup> poly(ethylene oxide) (PEO),<sup>43</sup> poly(dimethylsiloxane) (PDMS),<sup>43</sup> and poly(methylstyrene) (PMS),<sup>30</sup> and a variety of experimental techniques have been brought to bear. We have recently shown that all of the published data for hPB fall on a common curve ( $D$  versus  $M$ ) when reduced to a common temperature, and the resulting exponent is  $-2.30 \pm 0.05$  with a greater than 95% confidence interval.<sup>38</sup> These data extend beyond 400 entanglements per chain, an upper limit which far exceeds that achieved for other systems. This result therefore contradicts the prevailing belief that  $D \sim M^{-2.0}$ .<sup>2,3</sup> It is clearly of interest to compare this result with those for other polymers. Accordingly, we collected the available melt self-diffusion data for  $M/M_e \geq 3$  and plot them in Figure 14 as  $DM^2$  versus  $M/M_e$ . (We have deliberately omitted the data for polyethylene. Taken as a whole, they are numerically consistent with hPB, as expected, but they are considerably more scattered and often obtained on rather polydisperse materials.) Each data

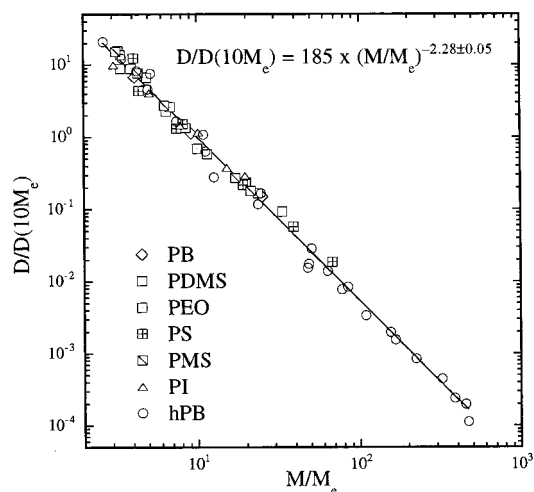


**Figure 15.** Melt self-diffusion (from Figure 14) normalized to the value at 10 entanglements per chain versus number of entanglements per chain.

set was fit to a power law, and the resulting exponents are indicated in the plot; these numbers therefore represent the apparent deviation from  $-2.0$ . With the exception of PI, all the data sets have an  $M$  dependence stronger than  $-2.0$ . (Other measurements for PI apparently also give much stronger exponents, however.<sup>71,72</sup>) If each of these seven data sets is normalized by the value of  $D(M=10M_e)$ , an excellent master curve is obtained, and the global fit gives an exponent of  $-2.28 \pm 0.05$ , as shown in Figure 15.<sup>38</sup> As the range of  $M/M_e$  is greatest for hPB, and because hPB represents almost 50% of the available data, the resulting exponent is heavily influenced by hPB. If the hPB data are excluded, a power law exponent of  $-2.17$  is obtained (not shown). In either case, the exponent is clearly stronger than  $-2.0$ .

The result implied by Figure 15 is sufficiently remarkable that it is appropriate to state clearly the conclusions we do and do not reach: (i) If one posits that the self-diffusion coefficient of a flexible, linear homopolymer chain in the melt scales with a *universal* power of molecular weight, then that exponent is  $-2.28 \pm 0.05$  within a 95% confidence limit. It is not  $-2.0$ . (ii) There is no clear evidence of a *universal* crossover to any other molecular weight dependence at higher molecular weight; there *may* be such a crossover beyond  $M/M_e > 10^2$ , but the available data are insufficient to either support or refute this conjecture. (iii) If there is a *nonuniversal* crossover to an exponent of  $-2.0$ , for hPB it occurs at or beyond  $M/M_e \approx 10^2$ , whereas for PS and PDMS it might occur near  $M/M_e \approx 10$ .

We do *not* infer that previous authors have misinterpreted or misrepresented their data, in concluding that their results support reptation or an exponent of  $-2.0$ . In many cases the deviation from  $-2.0$  was clearly noted but was generally attributed to CR processes at low  $M/M_e$ . This conclusion was well supported in some instances by extensive measurements of tracer diffusion in matrices of varying  $M$ .<sup>28,29</sup> In fact, all of the self-diffusion data might be well described by a combination of reptation plus CR, but our emphasis here is different. Rather than assume a particular model, we fit the entangled melt data to a power law, just as is generally done with  $\eta$ . The result is that when viewed from this perspective, the  $M$  dependences of  $D$  and  $\eta$  are essentially equivalent, and the longstanding anomaly

between the two exponents is resolved.<sup>38</sup>

**Comparison with Theory.** The  $M$  dependence of  $D$  for entangled melts is consistent with a power law exponent of  $-2.2$  to  $-2.3$ , and in entangled solutions the exponents fall between  $-2.3$  and  $-2.5$ . The reptation model predicts that the longest relaxation time,  $\tau_1$ , varies as

$$\tau_1 = \frac{L^2}{\pi^2 D_{\text{tube}}} = \left( \frac{N\zeta}{kT} \right) \left( \frac{N}{N_e} \right) \left( \frac{Nb^2}{\pi^2} \right) \quad (5)$$

where  $L$  is the tube length and  $b$  is the statistical segment length.<sup>2</sup> This, in turn, leads to the predictions

$$D = \frac{2R_g^2}{\pi^2 \tau_1} = \frac{1}{3} \left( \frac{kT}{N\zeta} \right) \left( \frac{N}{N_e} \right) \quad (6)$$

where Gaussian statistics are assumed ( $R_g^2 = Nb^2/6$ ), and

$$\eta = \frac{\pi^2}{12} \frac{\tau_1}{G_N} \quad (7)$$

Given that  $G_N$  is independent of  $M$  but varies approximately as  $\phi^2$ , as confirmed for our solutions,<sup>37</sup> eq 7 indicates that our experimental results for  $\eta$  imply  $\tau_1 \sim M^{3.4}\phi^{1.8}$ . This relation, when inserted into eq 6, implies that  $D \sim M^{-2.4}\phi^{-1.8}$ , which is in excellent agreement with the experimental results. (The chain dimensions are independent of  $\phi$  over this range, as shown by Westermann et al.<sup>73</sup>) It is in this sense that the solution diffusion and viscosity data are completely consistent. To pursue this more quantitatively, the following dimensionless ratio of experimental quantities can be formed:

$$\frac{D\eta}{R_g^2 G_N} = \frac{1}{6} \quad (8)$$

where the value of  $1/6$  is the bare reptation prediction. The results presented here are the first of which we are aware that provide experimental values of this ratio over a substantial range of  $\phi$  and  $M$  and that are independent of  $\phi$  and  $M$ . Utilizing the average values from Figures 6 and 8, and the relations  $G_N \approx 2.1 \times 10^6 \phi^2$  (Pa)<sup>37</sup> and  $R_g^2/M \approx 2 \times 10^{-17}$  (cm<sup>2</sup>),<sup>73</sup> we obtain 0.37, 0.44, 0.71, 0.72, 0.42, and 0.50 for hPB-10, hPB-20, hPB-50, dPB-100, h(d)PB-350, and dPB-420, respectively. The average value is 0.53, and the 95% confidence limit is  $\pm 0.3$ . This is approximately a factor of 3 larger than the bare reptation prediction and also of the PMC theory prediction (3/16).<sup>12</sup>

The concentration dependence of  $\eta$  has been examined experimentally by many workers in the concentrated regime,<sup>56</sup> with exponents typically in the range from 3.4 to 4, as found here.<sup>56</sup> For example, Colby et al. examined polybutadiene in two solvents all the way from dilute solutions to the melt and found  $\eta \sim \phi^{3.6}$  for  $\phi > 0.1$ .<sup>57</sup> (These data were carefully corrected for  $\zeta(\phi)$ .) Several different scaling predictions have been made for the  $\phi$  dependence of  $\eta$  and  $D$  for the concentrated regime, as follows:

$$\eta \sim N^3 \phi^x; \quad D \sim N^2 \phi^{-y} \quad (9)$$

with  $(x,y)$  being (3,1) from Doi and Edwards,<sup>2</sup> (3.5,1.5)

from Pearson,<sup>56</sup> and (14/3,7/3) from Colby, Rubinstein, and Daoud.<sup>74</sup> Superficially the predictions by Pearson appear closer to our experimental results, but this is potentially misleading. No matter the detailed assumptions that distinguish these three approaches, all assume bare reptation, and the values of  $x$  and  $y$  depend on the assumption of  $\tau_1 \sim N^3$ . Given that this assumption is not correct, any agreement between the data and the predicted  $\phi$  dependence has to be regarded as fortuitous. To examine the concentration dependence in more detail, we can write

$$\eta \sim \zeta \phi N \left( \frac{N}{N_e} \right)^{2+\delta}; \quad D \sim \frac{1}{\zeta} \frac{1}{N} \left( \frac{N_e}{N} \right)^{1+\delta} \quad (10)$$

where we have retained the two quantities that might depend on  $\phi$  (i.e.,  $\zeta$  and  $N_e$ ) and assuming that the chain dimensions do not. Equation 10 asserts that the difference between experiment and theory is due to a process (or processes) that depends only on the number of entanglements per chain, because  $\delta \approx 0.4$  not 0. This modification would alter the Doi–Edwards scaling prediction of  $(x,y)$  to (3.4,1.4),<sup>2</sup> which would be closer to, but still not consistent with, our experiments (assuming  $N_e \sim \phi^{-1}$ ). Similarly, both Colby–Rubinstein–Daoud exponents would increase and be even further from experiment.<sup>74</sup> The Pearson exponents, however, would become almost quantitatively correct, i.e., (3.9,1.9).<sup>56</sup> It is important, however, to consider how the Pearson treatment differs from that of Doi and Edwards. The latter attributes a Rouse-like friction to an entanglement length within the tube, i.e.,  $\zeta_e = \zeta N_e$ ,<sup>2</sup> whereas Pearson assumed a Zimm-like friction for the same entity,  $\zeta_e = \zeta \sqrt{N_e}$ . Although this approach appears to agree well with our experiments, it is not obvious that the Zimm-like friction is reasonable. First, over this  $\phi$  range the static correlation length,  $\xi$ , is less than 10 Å, and thus hydrodynamic interactions should be screened. (The tube diameter, which is the relevant length scale for  $\zeta_e$ , lies between 40 and 80 Å.) Second, the Pearson approach does not converge to the Doi–Edwards result in the melt, as the factor of  $\sqrt{N_e}$  would persist. The Doi–Edwards version would be closer to the experiments if, as suggested previously,  $N_e$  has a slightly stronger dependence on  $\phi$  than we obtained.<sup>2</sup> For example, if  $N_e \sim \phi^{1.2}$ , then the Doi–Edwards concentration exponents would become (3.9,1.7), which is certainly within the experimental uncertainty.

The preceding discussion establishes that the  $D$  and  $\eta$  results are consistent in their  $M$  and  $\phi$  dependences, as embodied in eq 8, and that the nonreptative  $M$  exponents are consistent with the  $\phi$  exponents. This second conclusion implies either that there is a stronger  $\phi$  dependence of  $N_e$  than we obtained or that the Zimm-like friction factor of Pearson is appropriate. A third possibility, as noted before, would be a mild  $\phi$  dependence to  $\zeta$ . We now turn to possible explanations for the  $M$  exponents. In the reptation framework, the enhanced  $M$  dependence of  $\eta$  has been attributed primarily to CLF,<sup>2</sup> as noted in the Introduction. The recent treatment by Milner and McLeish provides a more quantitative description of  $\eta(M)$ , which crosses over to the asymptotic  $M^3$  law above  $M/M_e$  of a few hundred.<sup>15</sup> It also yields a scaling of  $G'$  with  $\omega$  above  $\omega\tau_1 \approx 1$  that is closer to experiment than bare reptation. Apparently, also, the  $M$  dependence of  $D$  is similarly enhanced.<sup>27</sup> It may be, then, that CLF alone is sufficient to reconcile

the observed  $M$  dependence of  $\eta$  and  $D$ . However, it is abundantly clear from tracer diffusion measurements that matrix mobility plays an important role in self-diffusion,<sup>28–30</sup> and thus CR processes must be considered;<sup>4</sup> CLF should be independent of matrix molecular weight. Consequently, until CLF and CR are combined in one self-consistent modified reptation treatment, it is not really possible to ascertain how successful the model is.

Fetters and co-workers have recently suggested that the crossover to reptation exponents at very high  $M$  is not universal but in fact depends systematically on the packing length,  $p$ .<sup>75</sup> Interestingly, the inferred dependence is such that polymers with a low  $M_e$  (and thus lower  $p$ ) require many *more* entanglements before the asymptotic regime is achieved. None of the self-diffusion studies in Figure 14 traverse the predicted crossover, but PS and PDMS may actually come closer to doing so than hPB. As noted previously, the data for PS and PDMS do give some hint that the crossover occurs at a smaller  $M/M_e$  for these polymers. It would clearly be useful to make measurements on an appropriate system in order that this crossover can be accessed and thereby explore this prediction.

The polymer mode-coupling theory (PMC) of Schweizer and co-workers represents an ambitious attempt to capture the many-body dynamics of polymer liquids through a combination of liquid state theory for the structure of the fluid and the mode-coupling approach for the dynamics.<sup>9–12</sup> It is able to recover the asymptotic results of the reptation model without any explicit assumptions about the nature of chain motions. Furthermore, there are three identifiable finite  $N$  effects that can contribute to the experimentally observed exponents, associated with matrix chain motions, chain shape fluctuations, and spatial correlations among the entanglement constraints. The first two may be considered as analogous to CR and CLF, respectively, but the third is new. Its magnitude depends on the ratio of the static screening length to the entanglement spacing, and its influence becomes more important as solution concentration decreases. This provides a plausible mechanism for the small discrepancy between the  $M$  exponent for  $D$  in melts versus solutions. An extensive comparison of the predictions of this model with viscoelastic and transport properties of polymer melts and solutions has been given, and it is generally very successful.<sup>10,11</sup> Consequently one may anticipate that it can also describe the results presented here.

The reptation model is fundamentally a single-chain-in-a-mean-field approach, which is the origin of its simplicity. Other treatments begin with the opposite assumption, that cooperativity in the motions of several chains is the key feature of entangled chain dynamics. The model of Douglas and Hubbard<sup>8</sup> is a particularly intriguing representative of this class, but previous examples include the work of Bueche,<sup>76</sup> Fujita and Einaga,<sup>77</sup> Ngai and co-workers,<sup>6</sup> and Herman.<sup>7</sup> Douglas and Hubbard describe an “amoeba” model, in which clusters of entangled chains relax cooperatively to determine the long time dynamics, but this aspect is only a subset of a broader treatment of relaxation in condensed systems. The viscosity and diffusivity depend on  $M$  as power laws, with exponents that depend on the dimension of space ( $d$ ) and the fractal dimension of the chain (2 for Gaussian coils). The relevant results are

$$D \sim \frac{1}{M} \left( \frac{M}{M_e} \right)^{-4/d}; \quad \eta \sim G_N M_e^2 \left( \frac{M}{M_e} \right)^{2(d+2)/d} \quad (11)$$

which are in excellent agreement with the experimental  $M$  dependences. The  $\phi$  exponents depend on the  $\phi$  dependence of  $M_e$ . If  $M_e \sim \phi^{-1}$ , then the  $\phi$  exponents are  $-1.33$  for  $D$  and  $3.33$  for  $\eta$ , weaker than the experimental results. If  $M_e \sim \phi^{-1.2}$ , on the other hand, the results would be  $-1.6$  and  $3.8$ , respectively, in good agreement with the data. A key distinction between these predictions and those of reptation and the PMC, for example, is that in this case the crossover to reptation results occurs only in 4 dimensions, not in 3 dimensions at very high  $M$ . Thus, the presence or absence of a clear crossover to the reptation exponents at high  $M$  is a crucial issue, and as noted previously, the available diffusion data do not provide direct evidence of such a crossover. Unfortunately, the experiments necessary to explore this issue would be extremely difficult, as they would require an order of magnitude larger  $M$  samples than have been examined heretofore. Furthermore, as the diffusion results indicate, it might take several groups utilizing different samples and different techniques before one could be confident that a universal dependence had been established.

## Summary

We have described an extensive study of self-diffusion and viscosity in entangled solutions and melts of hydrogenated polybutadiene. The experimental results are consistent with  $D \sim M^{-2.4 \pm 0.1} \phi^{-1.8 \pm 0.2}$  and  $\eta \sim M^{3.4 \pm 0.1} \phi^{3.8 \pm 0.2}$ . The temperature dependences of both  $D$  and  $\eta$  are consistent and independent of  $\phi$  and  $M$ , implying (but not directly proving) that the monomeric friction factor is also independent of  $\phi$  and  $M$ . The relation  $M_e \sim \phi^{-1}$  was obtained previously and if precise suggests that there is a slight additional  $\phi$  dependence to the dynamics than embodied in  $(M/M_e)$ , which might be due to a correspondingly slight dependence to the monomeric friction factor. Alternatively, if  $M_e \sim \phi^{-1.2}$  is posited, in accordance with expectation for good solvent systems and not beyond the experimental uncertainty, then the experimental  $\phi$  dependence of  $D$  and  $\eta$  is entirely embodied in the dependence on  $(M/M_e)$ .

The most remarkable result is that the  $M$  exponent for  $D$  is not  $-2.0$ . The solution values here agree with all the (few) previous studies on well-entangled solutions and are centered about  $-2.4$  to  $-2.5$ . Our melt value is  $-2.4$ , but the data are in good agreement with several other measurements in hPB, and collected together the results are consistent with  $D \sim M^{-2.30 \pm 0.05}$ . The hPB melt data have also been compared to data on six other polymer systems. The data as a whole are consistent with a universal power law exponent of  $-2.28 \pm 0.05$ , with no obvious evidence of a crossover to  $-2.0$  at higher  $M/M_e$ ; the data extend to  $M/M_e \approx 450$ . It is not yet clear whether the stronger exponent in solution ( $-2.4$  to  $-2.5$ ) is significantly different from that in melts ( $-2.2$  to  $-2.3$ ), due to the uncertainty in the former. This exponent for diffusion is consistent with that for viscosity, in that the longest relaxation times defined by diffusion ( $\sim R_g^2/D$ ) and stress relaxation ( $\sim \eta/G_N$ ) have approximately the same  $M$  dependence, as predicted by most models. A longstanding anomaly in polymer dynamics is thus resolved.



The results are clearly not consistent with the bare reptation model, but recent treatments of contour length fluctuations can apparently reproduce the observed  $M$  exponents in both  $D$  and  $\eta$  and anticipate a crossover to the asymptotic reptation exponents at  $M/M_e$  of several hundred. However, extensive measurements of tracer diffusion reported by several groups indicate a matrix molecular weight dependence that is not attributable to contour length fluctuations; constraint release effects are assumed to be significant. Consequently, a remaining challenge for reptation theory is to incorporate both contour length fluctuations and constraint release in a self-consistent manner. The concentration dependence of both  $D$  and  $\eta$  is consistent with scaling arguments based on a mean-field approach, once the experimental  $M$  dependence is utilized in place of the predicted reptation exponent.

**Acknowledgment.** This work was supported by the National Science Foundation, through awards DMR-9528481 and DMR-9018807 to T.P.L. High-temperature SEC measurements by B. Chapman and P. Cotts are gratefully acknowledged. We benefited from helpful discussions with E. Kramer, T. McLeish, R. Colby, M. Rubinstein, K. Schweizer, J. Douglas, S. Milner, and H. Yu. J. Genzer and R. Composto provided valuable advice and assistance with the FRES experiments.

## References and Notes

- (1) de Gennes, P. G. *J. Chem. Phys.* **1971**, *55*, 572.
- (2) Doi, M.; Edwards, S. F. *The Theory of Polymer Dynamics*, 2nd ed.; Clarendon Press: Oxford, 1988.
- (3) Lodge, T. P.; Rotstein, N. A.; Prager, S. *Adv. Chem. Phys.* **1990**, *79*, 1.
- (4) Graessley, W. W. *Adv. Polym. Sci.* **1982**, *47*, 68.
- (5) Doi, M. *J. Polym. Sci., Polym. Phys. Ed.* **1983**, *21*, 667.
- (6) Ngai, K. L.; Rendell, R. W.; Rajagopal, A. K.; Teitler, S. *Ann. N.Y. Acad. Sci.* **1985**, *484*, 150.
- (7) Herman, M. F. *J. Chem. Phys.* **1990**, *92*, 2043.
- (8) Douglas, J. F.; Hubbard, J. B. *Macromolecules* **1991**, *24*, 3163.
- (9) Schweizer, K. S. *J. Chem. Phys.* **1989**, *91*, 5802, 5822.
- (10) Fuchs, M.; Schweizer, K. S. *Macromolecules* **1997**, *30*, 5156.
- (11) Fuchs, M.; Schweizer, K. S. *Macromolecules* **1997**, *30*, 5133.
- (12) Schweizer, K. S.; Fuchs, M.; Szamel, G.; Guenza, M.; Tang, H. *Makromol. Theory Simul.* **1997**, *6*, 1037.
- (13) Berry, G. C.; Fox, T. G. *Adv. Polym. Sci.* **1968**, *5*, 261.
- (14) Ferry, J. D. *Viscoelastic Properties of Polymers*, 3rd ed.; Wiley: New York, 1980.
- (15) Milner, S. T.; McLeish, T. C. B. *Phys. Rev. Lett.* **1998**, *81*, 725.
- (16) Tirrell, M. *Rubber Chem. Technol. Rubber Rev.* **1987**, *57*, 523.
- (17) Kim, H.; Chang, T.; Yohanan, J. M.; Wang, L.; Yu, H. *Macromolecules* **1986**, *19*, 2737.
- (18) Wheeler, L. M.; Lodge, T. P. *Macromolecules* **1989**, *22*, 3399.
- (19) Nemoto, N.; Kojima, T.; Inoue, T.; Kishine, M.; Hirayama, T.; Kurata, M. *Macromolecules* **1989**, *22*, 3793.
- (20) Nemoto, N.; Kishine, M.; Inoue, T.; Osaki, K. *Macromolecules* **1991**, *24*, 1648.
- (21) Komlos, M. E.; Callaghan, P. T. *J. Chem. Phys.* **1998**, *102*, 1648.
- (22) Rotstein, N. A.; Lodge, T. P. *Macromolecules* **1992**, *25*, 1316.
- (23) Colby, R. H.; Fetters, L. J.; Graessley, W. W. *Macromolecules* **1987**, *20*, 2226.
- (24) Rubinstein, M. *Phys. Rev. Lett.* **1987**, *59*, 1946.
- (25) Deutsch, J. M.; Madden, T. L. *J. Chem. Phys.* **1989**, *91*, 3253.
- (26) Reiter, J. *J. Chem. Phys.* **1991**, *94*, 3222.
- (27) Frischknecht, A.; Milner, S. *Macromolecules*, in press.
- (28) Green, P. F.; Mills, P. J.; Palmström, C. J.; Mayer, J. W.; Kramer, E. J. *Phys. Rev. Lett.* **1984**, *53*, 2145.
- (29) Green, P. F.; Kramer, E. J. *Macromolecules* **1986**, *19*, 1108.
- (30) Antonietti, M.; Coutandin, J.; Sillescu, H. *Macromolecules* **1986**, *19*, 793.
- (31) Nemoto, N.; Kishine, M.; Inoue, T.; Osaki, K. *Macromolecules* **1990**, *23*, 659.
- (32) Klein, J.; Fletcher, D.; Fetters, L. J. *Nature* **1983**, *304*, 526.
- (33) Bartels, C. R.; Crist, B.; Graessley, W. W. *Macromolecules* **1984**, *17*, 2702.
- (34) Crist, B.; Green, P. F.; Jones, R. A. L.; Kramer, E. J. *Macromolecules* **1989**, *22*, 2857.
- (35) von Seggern, J.; Klotz, S.; Cantow, H.-J. *Macromolecules* **1991**, *24*, 3300.
- (36) Pearson, D. S.; Fetters, L. J.; Graessley, W. W.; Ver Strate, G.; von Meerwall, E. *Macromolecules* **1994**, *27*, 711.
- (37) Tao, H.; Lodge, T. P.; Huang, C.-I. *Macromolecules* **1999**, *32*, 1212.
- (38) Lodge, T. P. *Phys. Rev. Lett.* **1999**, *83*, 3218.
- (39) Antonietti, M.; Coutandin, J.; Sillescu, H. *Makromol. Chem., Rapid Commun.* **1984**, *5*, 525.
- (40) Antonietti, M.; Fölsch, K. J.; Sillescu, H. *Makromol. Chem.* **1987**, *188*, 2317.
- (41) Green, P. F.; Palmström, C. J.; Mayer, J. W.; Kramer, E. J. *Macromolecules* **1985**, *18*, 501.
- (42) Fleischer, G.; Appel, M. *Macromolecules* **1995**, *28*, 7281.
- (43) Appel, M.; Fleischer, G. *Macromolecules* **1993**, *26*, 5520.
- (44) Fetters, L. J.; Lohse, D. J.; Richter, D.; Witten, T. A.; Zirkel, A. *Macromolecules* **1994**, *27*, 4639.
- (45) Rosedale, J. H. Ph.D. Thesis, University of Minnesota, 1993.
- (46) von Meerwall, E.; Beckman, S.; Jang, J.; Mattice, W. L. *J. Chem. Phys.* **1998**, *108*, 4299.
- (47) Vrentas, J. S.; Venerus, D. C.; Vrentas, C. M. *Chem. Eng. Sci.* **1991**, *46*, 33.
- (48) von Meerwall, E. D.; Burgan, R. D.; Ferguson, R. D. *J. Magn. Reson.* **1979**, *34*, 339.
- (49) von Meerwall, E.; Grigsby, J.; Tomich, D.; Van Antwerp, R. *J. Polym. Sci., Polym. Phys. Ed.* **1982**, *20*, 1037.
- (50) von Meerwall, E. D. *Adv. Polym. Sci.* **1983**, *54*, 1.
- (51) Mills, P. J.; Green, P. F.; Palmström, C. J.; Mayer, J. W.; Kramer, E. J. *Appl. Phys. Lett.* **1984**, *45*, 958.
- (52) Tirira, J.; Serruys, Y.; Trocellier, P. *Forward Recoil Spectrometry: Applications to Hydrogen Determination in Solids*; Plenum Press: New York, 1996.
- (53) Pearson, D. S.; Ver Strate, G.; von Meerwall, E.; Schilling, F. C. *Macromolecules* **1987**, *20*, 1133.
- (54) Raju, V. R.; Rachapady, H.; Graessley, W. W. *J. Polym. Sci., Polym. Phys. Ed.* **1979**, *17*, 1223.
- (55) Raju, V. R.; Menezes, E. V.; Marin, G.; Graessley, W. W.; Fetters, L. J. *Macromolecules* **1981**, *14*, 1668.
- (56) Pearson, D. S. *Rubber Chem. Technol.* **1987**, *60*, 439.
- (57) Colby, R. H.; Fetters, L. J.; Funk, W. G.; Graessley, W. W. *Macromolecules* **1991**, *24*, 3873.
- (58) Lodge, T. P. *Bull. Am. Phys. Soc.* **1998**, *43*, 204.
- (59) Green, P. F.; Doyle, B. L. *Macromolecules* **1987**, *20*, 2471.
- (60) Nicholson, J. C.; Crist, B. *Macromolecules* **1989**, *22*, 1704.
- (61) Hervet, H.; Léger, L.; Rondelez, F. *Phys. Rev. Lett.* **1979**, *42*, 1681.
- (62) Léger, L.; Hervet, H.; Rondelez, F. *Macromolecules* **1981**, *14*, 1732.
- (63) Wesson, J. A.; Noh, I.; Kitano, T.; Yu, H. *Macromolecules* **1984**, *17*, 782.
- (64) Callaghan, P. T.; Pinder, D. *Macromolecules* **1984**, *17*, 431.
- (65) Klein, J.; Briscoe, B. J. *Proc. R. Soc. London A* **1979**, *365*, 53.
- (66) Zupancic, I.; Lahajnar, G.; Blinc, R.; Reneker, D. H.; Vanderhart, D. L. *J. Polym. Sci., Polym. Phys. Ed.* **1985**, *23*, 387.
- (67) Peterlin, A. *Makromol. Chem.* **1983**, *184*, 2377.
- (68) Bachus, R.; Kimmich, R. *Polymer* **1983**, *24*, 964.
- (69) Fleischer, G. *Makromol. Chem., Rapid Commun.* **1985**, *6*, 403.
- (70) Fleischer, G. *Colloid Polym. Sci.* **1987**, *265*, 89.
- (71) Landry, M. R. Ph.D. Thesis, University of Wisconsin, 1985.
- (72) Park, S. Ph.D. Thesis, University of Wisconsin, 1992.
- (73) Westermann, S.; Willner, L.; Richter, D.; Fetters, L. J. *Makromol. Chem. Phys.*, in press.
- (74) Colby, R. H.; Rubinstein, M.; Daoud, M. *J. Phys. II* **1994**, *4*, 1299.
- (75) Fetters, L. J.; Lohse, D. J.; Milner, S. T.; Graessley, W. W. *Macromolecules* **1999**, *32*, 6847.
- (76) Bueche, F. *J. Chem. Phys.* **1952**, *20*, 1959.
- (77) Fujita, H.; Einaga, Y. *Polym. J.* **1985**, *17*, 1131.